

Note: This is an accepted in-press pre-proof peer-reviewed draft of the journal article:

Kathryn E. Rankin, Zoë J. Hazell, Angela M. Middleton, Mark N. Mavrogordato (2021)
“Micro-focus X-ray CT scanning of two rare wooden objects from the wreck of the London,
and its application in heritage science and conservation”. *Journal of Archaeological Science: Reports* 39, 103158

ISSN 2352-409X

DOI: <https://doi.org/10.1016/j.jasrep.2021.103158>

Available online 6th September 2021 at:

<https://www.sciencedirect.com/science/article/pii/S2352409X21003709>

1 **Micro-focus X-ray CT scanning of two rare wooden objects from the wreck of**
2 **the *London*, and its application in heritage science and conservation**

3
4 Kathryn E. Rankin^{a1}, Zoë J. Hazell^b, Angela M. Middleton^b, and Mark N.
5 Mavrogordato^a

6
7 ^aμ-VIS X-Ray Imaging Centre, Eustice Building (B5), Faculty of Engineering and
8 Physical Sciences, Highfield Campus, University of Southampton, SO17 1BJ, UK

9 ^bHistoric England, Fort Cumberland, Eastney, Portsmouth, Hampshire, PO4 9LD, UK

10
11 ¹ Corresponding author: k.rankin@soton.ac.uk

12
13 Zoe.Hazell@HistoricEngland.org.uk

14 Angela.Middleton@HistoricEngland.org.uk

15 mnm100@soton.ac.uk

16
17 *Abstract*

18 Two wooden objects, a tuning peg from a stringed musical instrument and a stopper
19 from a smoking pipe, were recovered from the AD 1665 wreck of the *London* and
20 selected for wood identification. So far, they are the only recoveries of these object
21 types from this wreck. To preserve their integrity and completeness, destructive
22 sampling was not desirable. Instead, micro-focus computed tomography (μ-CT)
23 scanning was carried out. The objects were scanned both pre-conservation
24 (waterlogged/saturated) and post-conservation (PEG impregnated; freeze-dried).
25 Although the aim was to non-destructively explore the internal structure of the
26 objects for wood identifications, information was also gained on their manufacturing
27 characteristics and internal condition. 1 μm voxel resolution – sufficient for positive
28 identifications of these wood types to genus level (as is standard for wood
29 identifications) – was achieved. This study has established that the conservation
30 treatment used here does not obscure the microscopic anatomical features of these
31 wood types and therefore recommends that μ-CT scanning is best undertaken after
32 conservation, when the objects are stable.

33
34 *Keywords*

35 Micro CT scanning; archaeological conservation; archaeological artefacts;
36 waterlogged wood; wood identification.

37 **1 Introduction**

38 The remains of the protected wreck of the *London* are located off Southend-on-Sea,
39 Essex, UK, where they have rested since it sank following an explosion in AD 1665.
40 In 2009 the wreck was put on the Heritage at Risk register (list entry 1000088) when
41 it was recognised that it was at risk of loss through erosion. To mitigate this risk, a
42 programme of surface recovery (by the licensed dive team) and limited excavations

43 (led by Cotswold Archaeology, funded by Historic England) took place from 2014–
44 2016. More than half of the recovered objects were wooden remains. These were
45 complemented by glass, ceramic, metal and other organic (leather, rope) materials
46 (see Walsh *forthcoming*). An extensive post-excavation phase – recording, analysing
47 and conserving the objects – has since followed, with material analysis adding a
48 valuable body of evidence to the archaeological record.

49

50 In heritage settings the need for sampling, especially invasive sampling, must be
51 carefully considered because archaeological artefacts are unique and non-
52 renewable. The removal of materials for analysis must be weighed up against
53 information gain, and such complex decisions often involve several stakeholders.
54 Guidance (Quye and Strlič 2019; *British Standard Institute* 2012) is available to
55 assist in decision-making through a series of questions, including, for example:
56 ‘Have non-invasive options been explored fully?’

57

58 In the case of the wooden material from the *London*, one of the main research aims
59 was to identify the types of wood (referred to here as ‘wood types’) used, by object
60 category. In most cases this was possible using the standard wood identification
61 technique of thin sectioning the wood to examine its microscopic anatomical
62 structure (see Hazell and Aitken 2019). As a destructive technique, where possible,
63 sub-samples were taken in already damaged or discreet areas.

64

65 However, options for studying rare and complete objects (here, a wooden pipe
66 stopper and the tuning peg from a stringed instrument) required more-careful
67 consideration. Options included i) no analysis, ii) invasive sampling and destructive
68 analysis of the sample, and iii) non-invasive analysis. Option i) *no analysis* was
69 discounted as the wood identification of these two rare examples from the
70 archaeological context would add valuable historical information to our
71 understanding of these object types. Option ii) was disregarded as both objects were
72 completely preserved, and sample taking from already damaged or discreet areas
73 was not achievable. Furthermore, any samples taken for thin-sectioning would be
74 large relative to the small object size. As the priority for these two objects was to
75 preserve them complete, option iii) *non-invasive analysis* was chosen.

76

77 A selection of non-destructive imaging techniques are available for use on wood,
78 each with its own merits (often relating to the wood’s preservation condition, be it
79 waterlogged, desiccated, mineralised, or charred), and not all suitable for wood
80 identifications (which depends on attaining spatial resolutions required to resolve
81 wood cellular structure). These include:

82

83 i) Scanning Electron Microscopy (SEM); see Cartwright (2015)

84 SEM is a surface imaging technique requiring destructive sampling and therefore not
85 suitable for the rare objects in this study.

86

87 ii) Magnetic Resonance Imaging (MRI); see Mori *et al* (2019) and Kanazawa *et*
88 *al* (2017),

89 Based on the nuclear magnetic resonance of hydrogen, MRI is suitable for
90 examining volumetric internal structure of waterlogged wooden objects, but is
91 typically lower resolution compared to μ -CT (Mori *et al* 2019, Morales *et al* 2004,
92 Kowalczyk *et al* 2019). Mori *et al* (2019) achieved 0.02 mm spatial resolution, which
93 would not enable smaller features such as perforation plates, pitting and spiral
94 thickenings to be resolved. Thus, MRI may be limited for the purpose of identification
95 of wood anatomy.

96

97 iii) Neutron tomography (NT); see Lehmann *et al* (2005),

98 NT has high sensitivity for detection of hydrogen, suiting it to inspection and
99 measurement of water and applied resin within wood. However, typical spatial
100 resolution of NT (20 μ m) would not be sufficient for identification of wood anatomy
101 without diffraction measurement of neutron scatter (Heacock *et al* 2020).

102

103 iv) Synchrotron radiation computed tomography (SRCT); see Mannes *et al*
104 (2010),

105 SRCT enables high resolution and high contrast volumetric imaging with high-
106 brilliance X-rays, making it significantly faster than lab sources. It has been
107 successful for multiple wood applications including anatomy identification for cultural
108 heritage applications (Mizuno *et al* 2010, Tazuru and Sugiyama 2019).

109

110 v) Lab-based micro-focus X-ray computed tomography (μ -CT) (see below).

111 μ -CT is more readily accessible than SRCT, with image contrast primarily
112 determined by variation in X-ray absorbance (Landis and Keane 2010). This may
113 result in low contrast to noise ratio (CNR) between wood and water-saturated areas
114 (O'Connor 2007, p. 46). Here, μ -CT was trialled as a non-destructive volumetric
115 analysis tool to image the internal structure of the two objects. This technique has
116 been successfully used on wood previously (Steppe *et al* 2004; Wei *et al* 2011) with
117 multiple cultural and heritage applications for wooden objects, for example:

118 i) on individual musical instruments (Fioravanti *et al* 2017, Van den Bulcke *et al*
119 2017),

120 ii) on archaeological remains for wood identifications e.g. on wood charcoal (Bird
121 *et al* 2008, Hubau *et al* 2013), on mineralised wood (Haneca *et al* 2012)
122 and/or dendrochronological studies (Grabner *et al* 2009, Stelzner and Million
123 2015), and

124 iii) for experimental studies determining internal degradation e.g. fungal decay
125 (Van den Bulcke *et al* 2008, Hervé *et al* 2014).

126 Prior μ -CT studies destructively sampled sections of wood for μ -CT. Here, μ -CT is
127 conducted on complete objects in the waterlogged and conserved state for wood
128 identification and internal integrity assessment.

129 **2 The wooden objects**

130 Following their recovery, the objects underwent desalination and conservation at
131 Historic England's conservation facilities at Fort Cumberland, Portsmouth (Section
132 3.1). Two objects not to be destructively sampled were selected for μ -CT scanning to
133 investigate their internal structure, primarily to determine the wood types:

134

- 135 • Pipe stopper (SF3342) (Figure 1A)

136 A decorated stopper for use with a smoking pipe, probably used to tamp down
137 tobacco. It is complete, but in two pieces: the head and the shaft. At its
138 maxima, the head is 30.5 mm wide and 13.7 mm deep, and the shaft is 23.2
139 mm long, with 9.4 mm diameter at the lower end. When complete, it would
140 have been approximately 56 mm tall.

141

- 142 • Tuning peg (SF3730) (Figure 1B)

143 A tapered tuning peg from a stringed musical instrument: 59.2 mm total length
144 and 14.8 mm wide at the head (the finger grip). The shaft is conical, 39.7 mm
145 long, with a taper of 2.6 degrees and a hole (1.7 mm diameter) for the string,
146 centred approximately 17.0 mm from the tip. On close examination whilst still
147 waterlogged, a circular insert (2.6 mm diameter at the surface) of a different,
148 paler-coloured unknown material was observed on the top edge of the head,
149 likely as decoration.

150

151 (Reported dimensions from μ -CT data of the conserved objects (see Section 3.4.4)).

152

153 Figure 1. Photographs (post-conservation) of (A) the pipe stopper, showing the head
154 section at the top left and the shaft section at the bottom right of the image, and (B)
155 the tuning peg, with the head section (finger grip) on the left and the shaft section on
156 the right of the image.

157



157

158 **2.1 Decay and conservation treatments of waterlogged wood**

159 As soon as it enters the ground or the water, wood, a natural material, is subject to
160 biodegradation. Compared to terrestrial sites, wood is normally better preserved in
161 waterlogged environments, due to lower oxygen levels which slow down fungal and

162 bacterial decay processes. Wood decay in wet/waterlogged environments, as in the
163 case of the *London*, is mainly caused by soft rot fungi, and/or by tunnelling-, erosion-
164 or cavity-bacteria (Hocker 2018, p. 13, Hoffman 2013, p. 26). Microorganisms
165 preferentially degrade the cellulose rich secondary layers of the wood cell wall,
166 leaving the lignin rich middle lamella behind. Additionally, in the marine environment
167 marine wood borers (*Teredo* and *Limnoria* species) burrow channels into the wood.
168 Decay starts on the outside and over time moves into the centre of the wood,
169 resulting in a more decayed outer layer and better-preserved inner section (Hoffman
170 2013, p. 27). Both micro- and macroscopic damage removes wood substance,
171 resulting in a physically weakened and soft material. Gaps created in the cell wall
172 due to microscopic decay are filled with water, which supports the weakened wood
173 cell structure and at the same time preserves the wood's overall shape and
174 dimension.

175

176 As a result of material loss, waterlogged archaeological wood can rarely be dried
177 without a pre-treatment (Hocker 2018, p. 69) and requires a more interventive
178 approach. All wood conservation techniques have the same overall goal: to remove
179 water from within the wood cell structure whilst limiting dimensional changes. This is
180 normally achieved by impregnation followed by drying. A number of materials have
181 been used for impregnation, such as sugars, or synthetic materials such as
182 Kauramin (a melamine resin) or PEG (polyethylene glycol). Drying methods can
183 include slow air-drying or vacuum freeze-drying. It is worthwhile mentioning that
184 some dimensional changes are inevitable as wood transitions from waterlogged to
185 dry.

186

187 The conservation methods selected here were impregnation with PEG followed by
188 vacuum freeze-drying, which is a well-established and commonly-used combination
189 approach. Examples include small finds from the shipwrecks of the *Vasa* and *Mary
190 Rose* (Hocker 2018, p. 69; Jones 2003, p. 64). PEG fulfils the role of a bulking agent
191 by providing support to the wood cell structure, ensuring that the overall shape and
192 dimensions are preserved. PEG is available in different grades, ranging from liquid to
193 solid. Using two different grades (liquid/ low and solid/ high molecular PEG) provides
194 support through bulking across well- and less well-preserved areas of wood,
195 respectively (Hoffman 2013, p. 59). PEG also has very good aging properties (Jones
196 2003, p. 64). Vacuum freeze-drying is a slow and gentle drying technique which
197 avoids the liquid phase of water and thereby circumvents surface tension of water
198 when it evaporates (Flink and Knudsen 1983), which would be strong enough to
199 cause cell collapse (shrinking, splitting and warping) if archaeological wood were to
200 air-dry (Barbour 1990, p. 187).

201

202 **3 Methods**

203 **3.1 Conservation of the pipe stopper and the tuning peg**

204 First, the objects underwent desalination to remove soluble salts. This involved
205 frequent water changes using distilled water and checking the conductivity of the
206 storage water (Cronyn 1990, p. 81). Once the conductivity had plateaued, active
207 conservation was implemented. Prior to PEG treatment, the objects were μ -CT
208 scanned (Section 3.3).

209

210 Wooden objects were submerged in 30% PEG 400 (low molecular) (volume by
211 volume) for three months and 30% PEG 4000 (high molecular) (weight by volume)
212 for another three months. They were then pre-frozen at -30°C in a domestic chest
213 freezer for one week, before being freeze-dried in a LyoDry Midi Freeze Dryer s/n
214 F012. The chamber temperature was set at -30°C and the condenser temperature
215 was set to -45°C . The removal of water via sublimation during the vacuum freeze-
216 drying process was monitored by weighing the objects. The endpoint was
217 determined when the weight-loss plateaued. Excess PEG was carefully removed
218 from the wood surface after freeze-drying, using brushes and wooden skewers. The
219 objects were then CT-scanned (Section 3.4).

220

221 **3.2 μ -CT Scanners**

222 Lab μ -CT scanner selection was first governed by scan time criteria, set for the
223 waterlogged objects to keep scans as short as possible to minimise drying. The first
224 aim was to obtain the full geometry ('overview') of the object in one scan, at the
225 highest resolution possible i.e. filling the field of view (FOV). For these faster, lower
226 resolution overview scans, a modified 225 kVp (225 W) Nikon/X-tek HMX μ -CT
227 scanner (Nikon metrology, UK) ('HMX') with a Perkin Elmer XRD 1621 CN14 HS
228 detector (PerkinElmer Optoelectronics, Germany) and Tungsten reflection target
229 material was selected. This scanner is capable of a range of spatial resolutions
230 ranging from 3 microns (6 mm FOV) to 55 microns (110 mm FOV).

231

232 Once the objects were conserved and dried, the time criteria were removed enabling
233 longer scan times for identification of micron-scale anatomical features within a
234 region of interest (ROI) at higher spatial resolution. A 160 kVp (10 W) Zeiss Xradia
235 Versa 510 X-ray microscope CT scanner (Carl Zeiss Microscopy GmbH, Germany)
236 ('Versa') with a transmission target was selected. This scanner is capable of sub-
237 micron (~ 600 nm) spatial resolution with two stage magnification; primary
238 magnification is geometrical from the X-ray cone beam and source-to-object/source-
239 to-detector distances (SOD/SDD), and secondary magnification occurs post-
240 scintillation as optical microscope objective lenses further magnify the image ahead
241 of the charged-coupled device (CCD) detector (Appendix Figure A1).

242

243 **3.3 μ -CT of waterlogged wooden objects (pre-conservation)**

244 Each object was removed from water prior to scanning and mounted in polymer
245 foam within a polymer beaker, sealed with Parafilm™ to minimise drying.

246 **3.3.1 Pipe stopper**

247 The pipe stopper was scanned in the HMX at 100 kVp peak voltage and 40 W
248 power, with an SOD of 88.4 mm and an SDD of 755.0 mm. Using an analogue gain
249 of 24 dB and binning 1 of the detector, 2801 and 1601 projection images were
250 acquired throughout 360 degrees rotation of the head and shaft pipe stopper
251 sections, respectively, averaging 8 frames per projection (FPP) with 134 ms
252 exposure time per frame. The head and shaft sections were scanned separately to
253 maximise the voxel (volume element or cubic pixel) resolution achievable.

254 **3.3.2 Tuning peg**

255 The tuning peg was scanned in the HMX at 80 kVp and 45 W, with an SOD of 127.0
256 mm and an SDD of 704.0 mm. With 18 dB analogue gain and binning 1, 1201
257 projection images were acquired, averaging 4 FPP with 134 ms exposures.

258 **3.3.3 Data preparation**

259 Projection images from the HMX were reconstructed into 32 bit float volumetric
260 datasets using filtered back-projection algorithms implemented within CTPro3D and
261 CTAgent software v2.2 (Nikon Metrology, UK). The resulting voxel resolution was
262 23.4 μ m and 36.1 μ m for the pipe stopper and tuning peg, respectively. Each 32 bit
263 raw volume was down-sampled to 8 bit using ImageJ/Fiji (Rasband, W.S., ImageJ,
264 U. S. National Institutes of Health, Bethesda, Maryland, USA,
265 <https://imagej.nih.gov/ij/>, 1997-2019) to reduce data processing time.

266

267 **3.4 μ -CT of conserved wooden objects (post-conservation)**

268 The conserved objects were scanned at higher resolution using the Versa scanner,
269 with the aim of making specific identifications of wood type by achieving the best
270 spatial resolution possible (sub-micron).

271 **3.4.1 Pipe Stopper**

272 The shaft of the pipe stopper was selected for this scanning phase, to minimise the
273 X-ray penetration path length and thus maximise the possible signal-to-noise ratio
274 (SNR). The shaft was wrapped in Parafilm™ and mounted in a thin-walled polymer
275 tube on an aluminium base. A two stage approach first located an ROI within the
276 shaft (i.e. in a representative area which was not cracked or excessively degraded)
277 (Stage 1) and then scanned at sub-micron resolution (Stage 2), using parameters
278 outlined in Table 1. The voxel resolutions achieved in the first and second scan
279 stages were 3.0 μ m and 0.7 μ m from approximately 2.5 hours and 75 hours
280 acquisition time, respectively.

281

Object	Scan Stage	Peak Voltage (kV)	Power (W)	SOD (mm)	SDD (mm)	Obj.	Bin.	Exp. (s)	Proj. / FPP	Voxel Resolution (μm)
Pipe Stopper	1	80	7	16.1	36.5	4X	2	1	3201 / 1	3.0
	2	80	7	16.1	30.5	20X	2	32	8001 / 1	0.7
Tuning Peg	0	80	7	16.1	136.1	0.4X	2	1	801 / 1	8.2
	1	80	7	16.1	36.5	4X	2	1	3201 / 1	3.0
	2	80	7	16.1	30.5	20X	2	32	8001 / 1	0.7
	3	80	7	16.9	108.1	4X	2	5	6001 / 1	1.0

282

283 Table 1. The μ -CT parameters used for scanning the conserved pipe stopper shaft
 284 and tuning peg. SOD = source-to-object distance, SDD = source-to-detector
 285 distance, Obj. = magnification objective, Bin. = binning, Exp. = exposure time, Proj. =
 286 number of projection images, and FPP = frames per projection.

287

288 3.4.2 Tuning Peg

289 The tuning peg was mounted in the same tube as the pipe stopper, but with the
 290 addition of low-density floral foam at the base and a collar of Parafilm™ at the top of
 291 the tube, to minimise movement. A multi-stage scanning approach (Table 1) was
 292 used to first locate the circular insert ROI and a secondary ROI within the main body
 293 of the peg itself, at lower resolution (8.2 μm voxel resolution) (Stage 0), before
 294 following the protocol used to scan the pipe stopper (Stages 1 and 2). An additional
 295 scan (Stage 3) was performed at 1.0 μm voxel resolution, as a compromise in
 296 resolution, FOV, and exposure time, which could be reduced due to the increase in
 297 flux with the 4X objective, thus reducing scan time (to approximately 11 hours).

298

299 3.4.3 Data preparation

300 The projection data from the Versa was reconstructed using the Zeiss XM
 301 Reconstructor software (Carl Zeiss Microscopy GmbH, Germany) into 16 bit TXM
 302 files then converted to 16 bit raw volumes.

303 3.4.4 μ -CT overview scans of conserved objects

304 Finally, the objects were also scanned in the HMX scanner again to evaluate the full
 305 geometry once conserved using the parameters in Table 2. The head and shaft of
 306 the pipe stopper were scanned individually, and four scans were acquired to cover
 307 the overall height of the tuning peg at higher resolution. The same reconstruction
 308 method was used as in Section 3.3.3, to give 8 bit raw volumes, which were then
 309 concatenated.

310

Object	Peak Voltage (kV)	Power (W)	SOD (mm)	SDD (mm)	Analogue Gain (dB)	Bin.	Exp. (ms)	Proj. / FPP	Voxel Resolution (μm)
Pipe Stopper head	80	28	83.2	749.5	24	1	250	2801 / 8	22.2
Pipe Stopper shaft	80	28	83.2	749.5	24	1	250	1201 / 8	22.2
Tuning Peg	80	20	39.3	797.9	24	1	354	1501 / 8	9.9

311 Table 2. The μ -CT parameters used for scanning the conserved objects within the
312 HMX to evaluate full geometry.

313

314 3.5 Wood identifications

315 The wood was identified using the identification texts and keys by Schweingruber
316 (1990), Schoch *et al* (2004) and Gale and Cutler (2000). Standard identifications
317 involve recording features seen on the three planes: transverse section (TS), radial
318 longitudinal section (RLS) and tangential longitudinal section (TLS).

319

320 Identification attempts were made using the pre- and post-conservation μ -CT
321 volumes. Each raw volume was imported into VGStudioMax v2.1 (Volume Graphics
322 GmbH, Germany) with an *xyz* co-ordinate system. The volumes were reorientated to
323 align the orthogonal planes (*xy*, *xz* and *yz*) with the TS, RLS, and TLS planes so that
324 they could be inspected for microscopic wood anatomical features. To achieve
325 secure identifications, it was necessary to locate key small characteristics such as:
326 ray width and ray cell type, perforation plates and spiral thickenings. In the case of
327 the perforation plates, the volumes had to be further re-orientated to see them in
328 plane (Figure 6). Typically, this meant tilting by 30–45° (relative to each vessel's
329 axis).

330

331 4 Results and Discussion

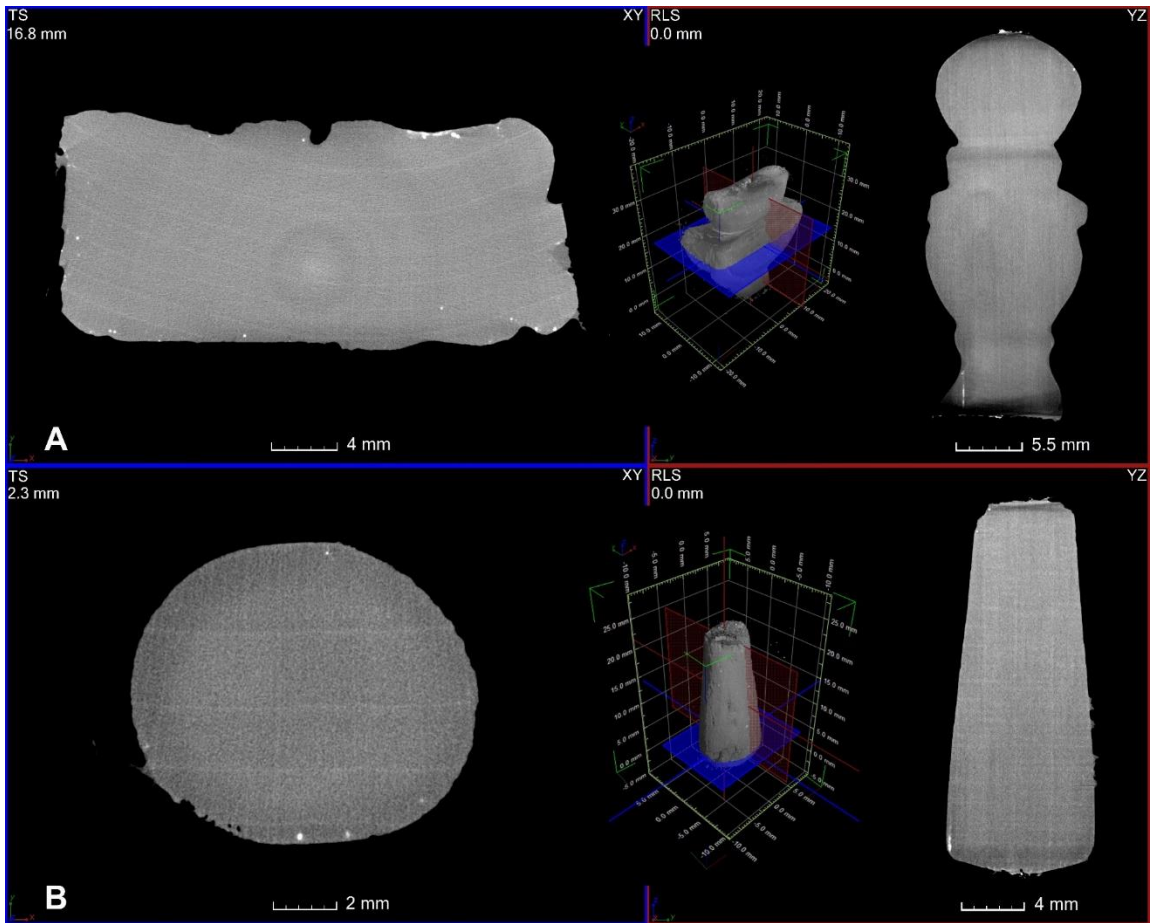
332 4.1 Pre-conservation

333 4.1.1 Pipe stopper

334 The results of the pre-conservation μ -CT of the pipe stopper are illustrated in Figure
335 2 (with head 3D rendering in Appendix Figure A2). The concentric rings are a CT
336 artefact, known as ring artefacts (Barrett and Keat 2004) and are more visible post-
337 conservation (Figure 13). These originate from consistent false signals from some
338 pixels on the detector that, when reconstructed from 360 degrees of projection data,
339 become a ring in the plane perpendicular to the axis of rotation.

340

341 Figure 2. Slice data through the TS (blue plane) and RLS (red plane) of the pipe
 342 stopper, before conservation (HMX): (A) upper piece (head), and (B) lower piece
 343 (shaft).



344
 345

346 On the pre-conservation (wet/waterlogged) μ -CT scans it was possible to identify
 347 growth ring boundaries. On the head of the pipe stopper, the ring boundaries were
 348 aligned approximately parallel with the longest face of the object (Figure 2(A)). Whilst
 349 the structural elements required for a secure wood identification were not adequately
 350 resolved due to low CNR, it was possible to identify it as an angiosperm (hardwood)
 351 and discount certain distinctive wood types with larger, characteristic features (e.g.
 352 those with a ring porous vessel structure such as *Quercus* sp. (oak)).

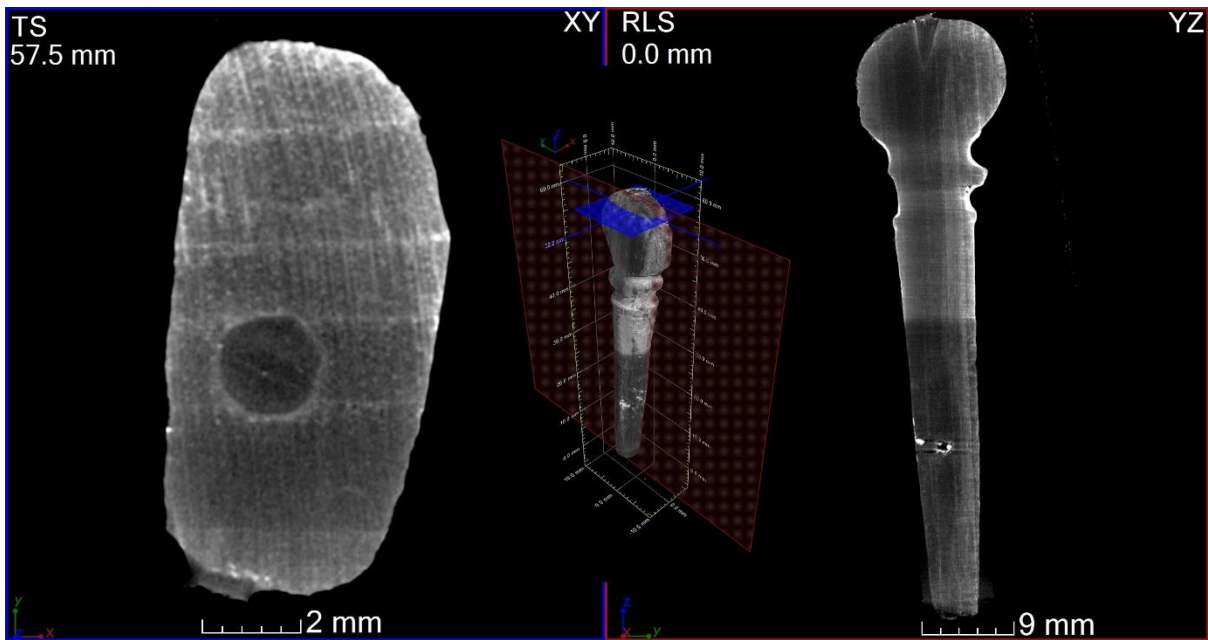
353

354 4.1.2 Tuning peg

355 The results of the pre-conservation scanning of the tuning peg are presented in
 356 Figure 3 (with 3D rendering in Appendix Figure A3). It can be seen that the circular
 357 insert on the top edge of the head (finger grip) was in fact a conical insert set 5 mm
 358 into the main body of the tuning peg.

359

360 Figure 3. Slice data through the TS (blue plane) and RLS (red plane) of the tuning
 361 peg, before conservation (HMX).



362
363

364 On the body of the tuning peg it was possible to resolve growth rings, but the exact
365 number of rings was uncertain due to limited image contrast. Overall, the wood
366 looked to be an angiosperm (hardwood), with faint suggestion that the rays could be
367 multiseriate. On the head section (the finger grip) the growth ring boundaries were
368 aligned perpendicular to its longest edge. It was also just possible to distinguish
369 growth rings on the decorative cone insert confirming it to be wood rather than
370 another material (e.g. shell/bone).

371

372 **4.2 Post-conservation**

373 The scans on the Versa achieved sub-micron spatial resolution, such that the wood
374 anatomical features required for a secure identification were visible.

375 **4.2.1 Pipe stopper**

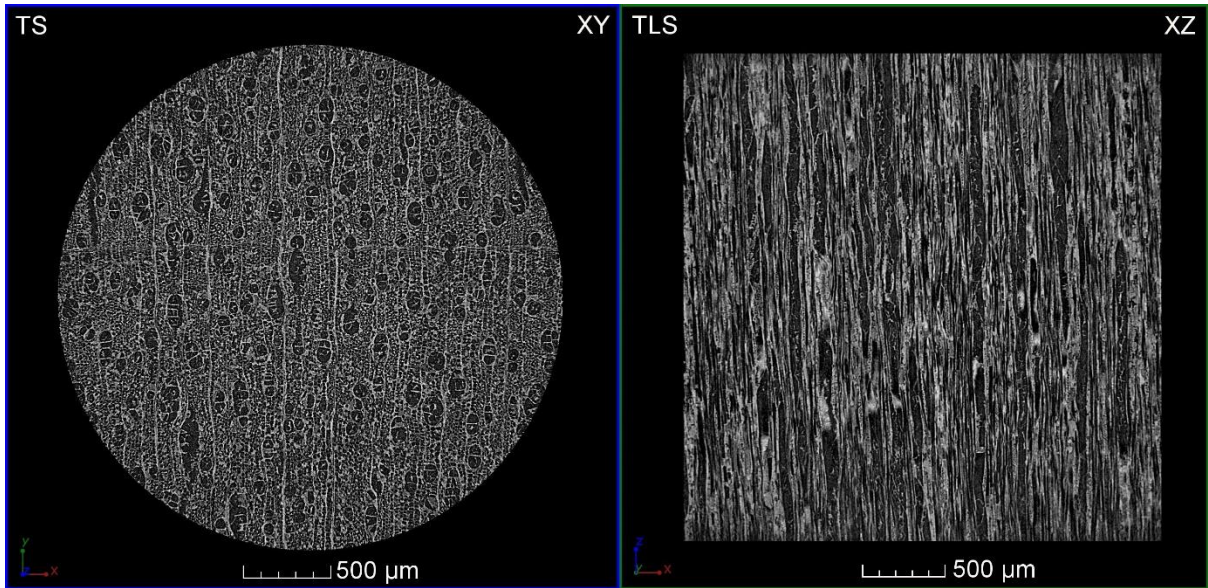
376 The wood is identified as a *Betula* sp. (birch), from the combination of the following
377 features: i) diffuse porous alignment of vessels with short radial chains (Figures 4
378 and 5 (TS)), ii) the presence of scalariform perforation plates generally with more
379 than 10 narrowly-spaced bars (Figure 6), iii) multiseriate rays (Figure 5) and iv)
380 absence of aggregate rays. Additionally, although the individual vessel pits (~1 μm)
381 were not fully resolved, their alignment which formed an overall 'fingerprint'-like
382 pattern was seen (Figure 5); this is a characteristic frequently seen by the specialist
383 (ZJH) in other material of this wood type.

384

385 From the post conservation 'overview' μ-CT volume on the HMX, it was possible to
386 clearly identify and distinguish growth rings in the head section of the pipe stopper.

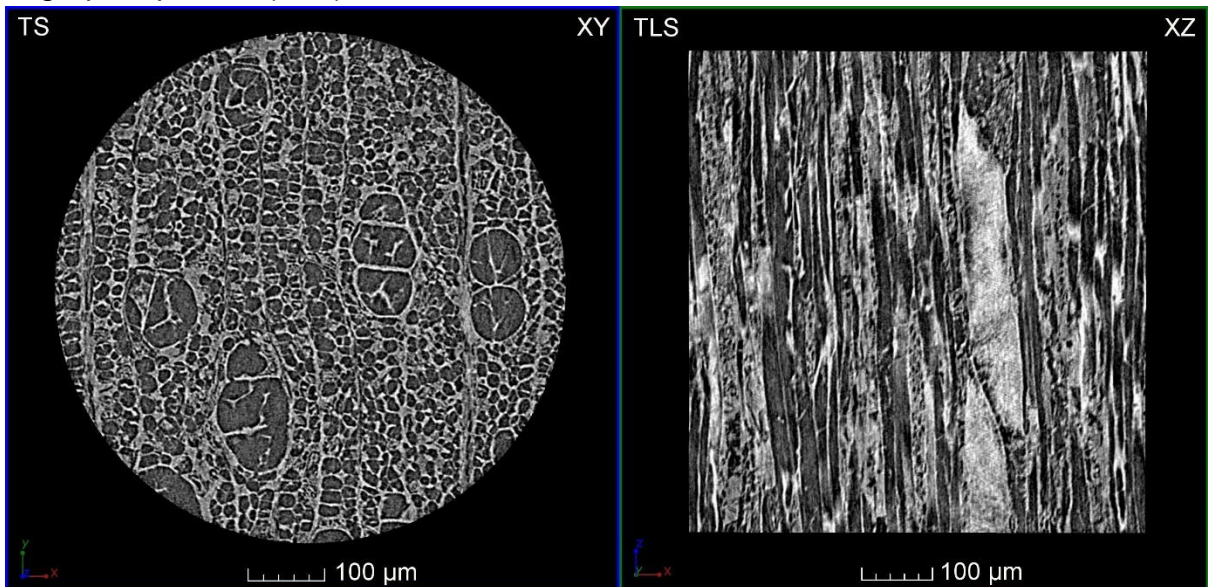
387

388 Figure 4. Post conservation (Versa) pipe stopper Stage 1: Slices through the TS
389 shows a growth ring boundary and vessels with short radial chains, but in the TLS, 3
390 μm voxel resolution was insufficient to resolve the detail of the ray cells.



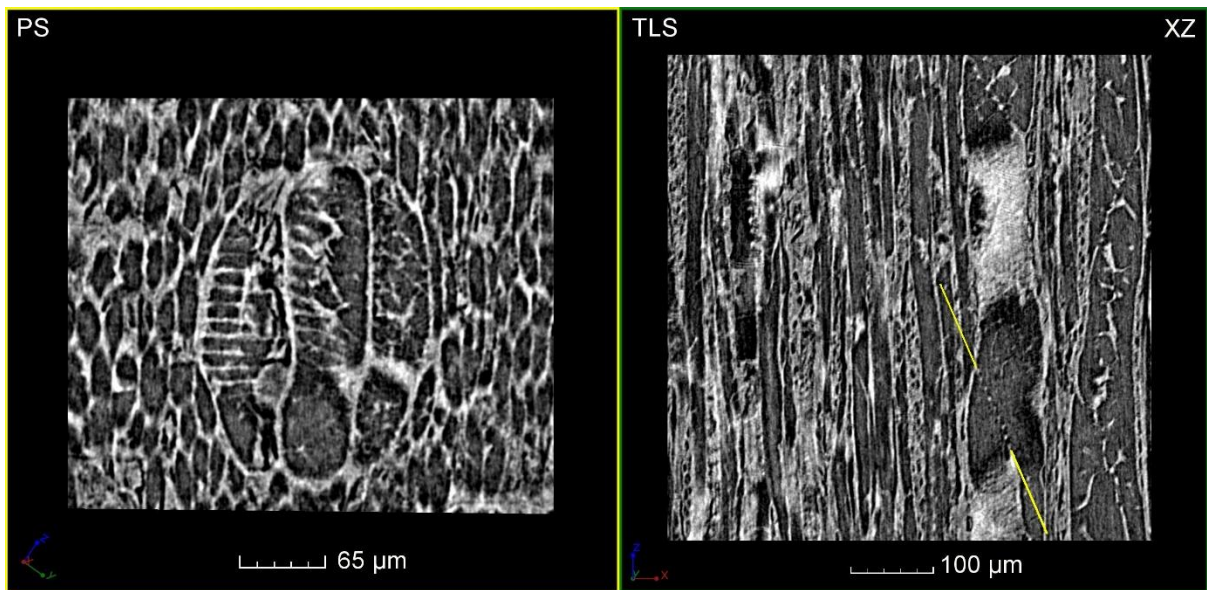
391
392
393
394
395
396

Figure 5. Post conservation (Versa) pipe stopper Stage 2: Slices through the volume
at 700nm voxel resolution show short radial chains (TS), multiseriate rays (TLS) and
fingerprint pattern (TLS).



397
398
399
400
401
402

Figure 6. Post conservation (Versa) pipe stopper Stage 2: At 700nm voxel resolution,
the bars of the scalariform perforation plates are clearly resolved. Here, the volume
has been re-orientated to view the plate face-on (left) as a planar section (PS)
indicated by the yellow plane location in the TLS side-on view.



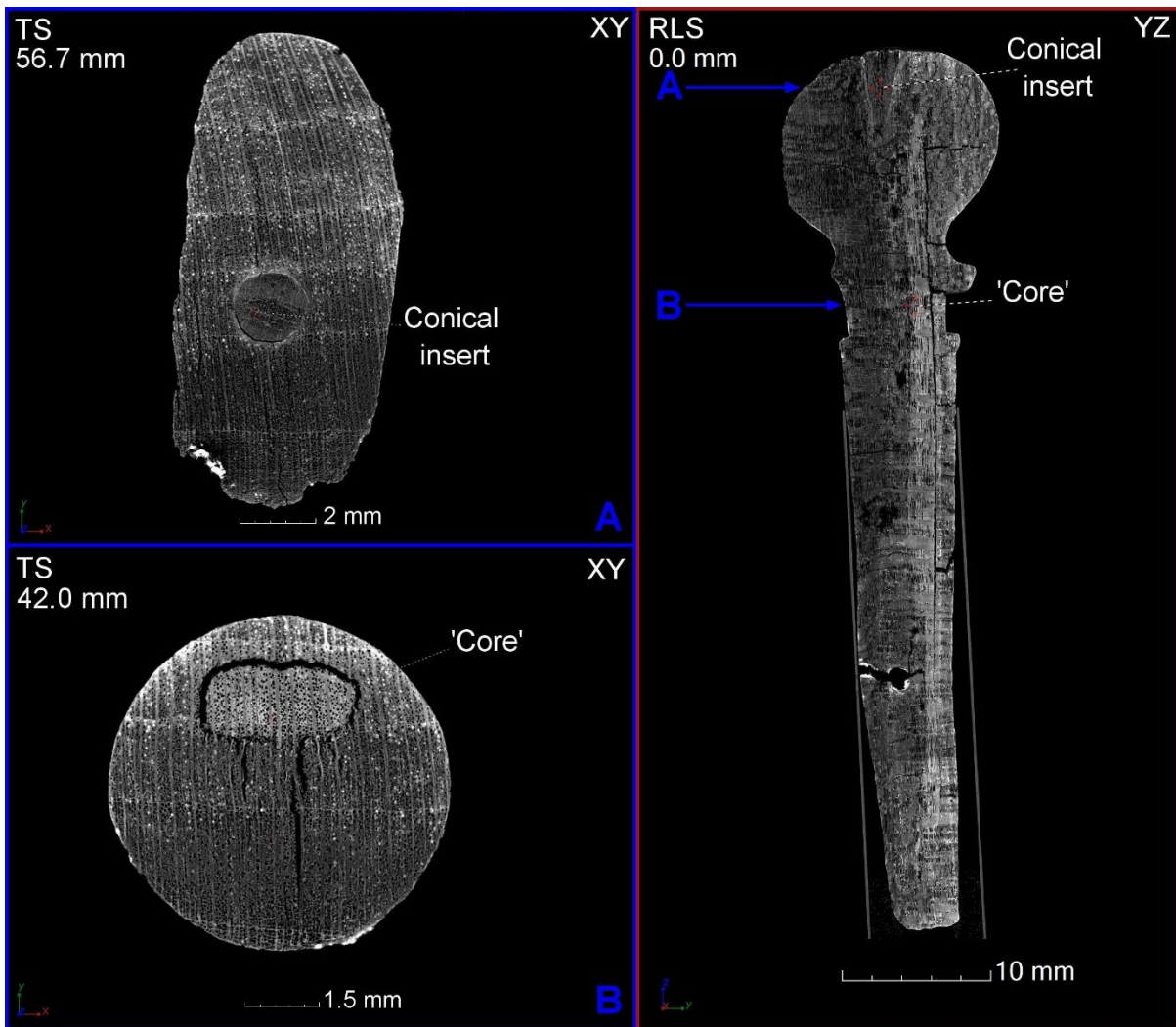
403
404

405 **4.2.2 Tuning peg**

406 The conical insert (Figure 7) was made from wood – a gymnosperm: softwood,
407 conifer – which differed from the main peg (an angiosperm: hardwood).

408

409 Figure 7. Post conservation (HMX) tuning peg overview scan: Slices showing the
410 location in the RLS (right) of the decorative conical insert A (viewed in the TS plane,
411 left) and inner 'core' B (viewed in the TS plane, left). Note the semi ring porous
412 vessel distribution in the TS.



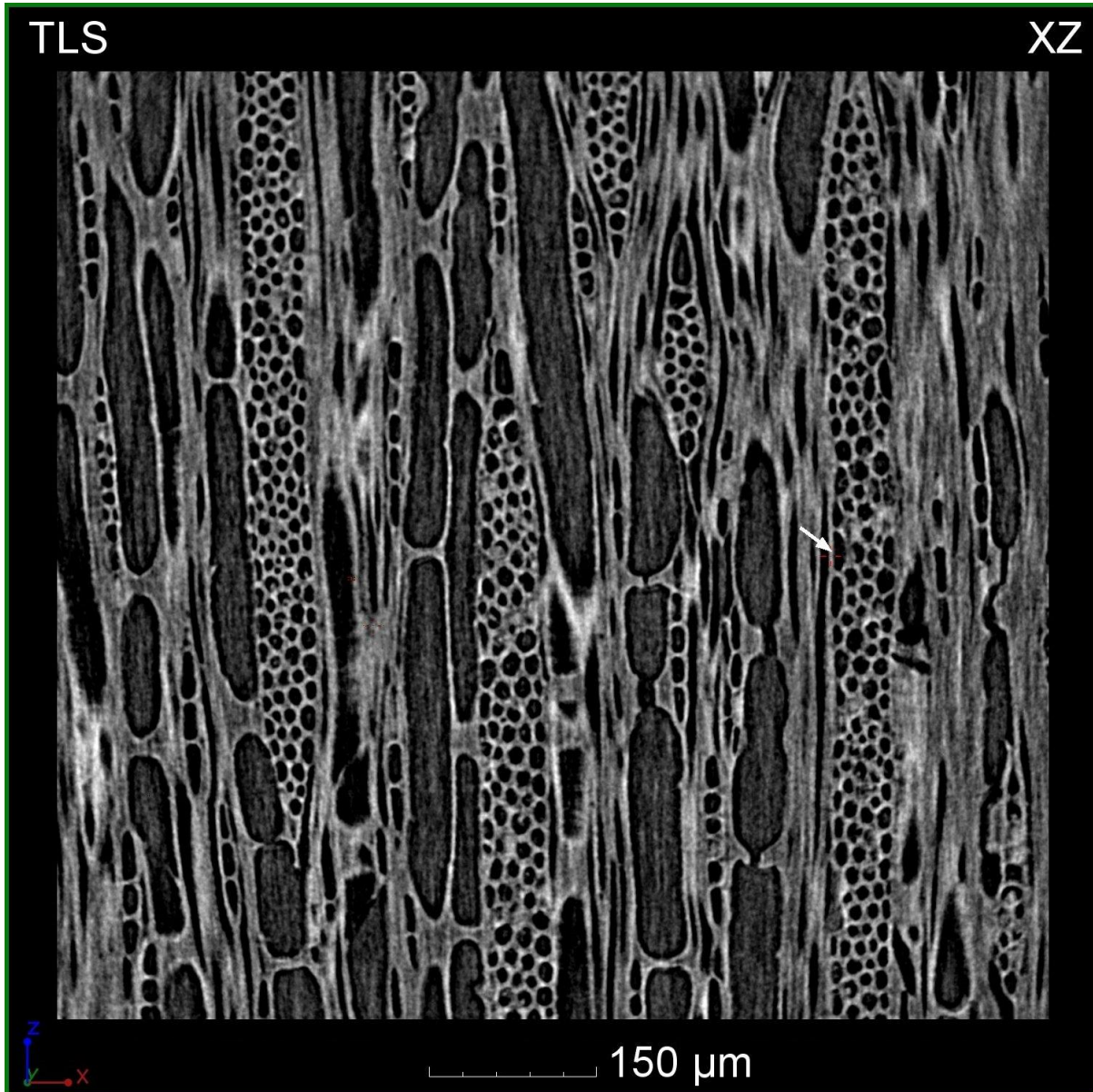
413
 414
 415
 416
 417
 418
 419
 420
 421
 422
 423
 424
 425
 426
 427
 428
 429
 430
 431
 432

The μ -CT scanning showed that the body of the tuning peg has an inner ‘core’ of better-preserved wood aligned longitudinally through it. For the most part, this ‘core’ is separate (i.e. internally detached) along its length, and is only attached at the top and bottom of the object (Figure 12). This ‘core’ was used for the wood identification of the peg body. It was identified as a *Prunus* sp. (the cherries genus) with: i) semi-ring porous vessel pattern (Figure 7), ii) noded rays at the ring boundary, iii) rays up to 5 cells wide and up to 80 cells (c 1.5mm) high (Figure 8), and iv) the presence of distinct spiral thickenings (Figure 9). Anatomically, the *Prunus* species are very similar and so resolving to species (which is possible in some cases) has been inhibited here by not being able to achieve sufficient spatial resolution. Unfortunately, in spite of two attempts, scan Stage 2 (0.7 μ m voxel resolution) was unsuccessful due to this object’s instability. Despite this, it was possible to confidently discount *P. avium* (wild cherry), as the ray heights of that species are too short (Schweingruber 1990, p. 138). Based on ray cell heights observed here (up to c. 80), a *P. spinosa* (blackthorn) type is possible, which is a group that also includes *P. cerasifera* (cherry plum), *P. domestica* (wild plum), *P. insititia* [= *P. domestica* ssp. *insititia*] (damson) and *P. persica* (peach) (see Schoch et al 2004; <http://www.woodanatomy.ch/species.php?code=PNPE>). The observation in the

433 sample material of some degree of ray cell heterogeneity (sheath cells were
434 observed in places (Figure 8)) would also fit with this group.

435

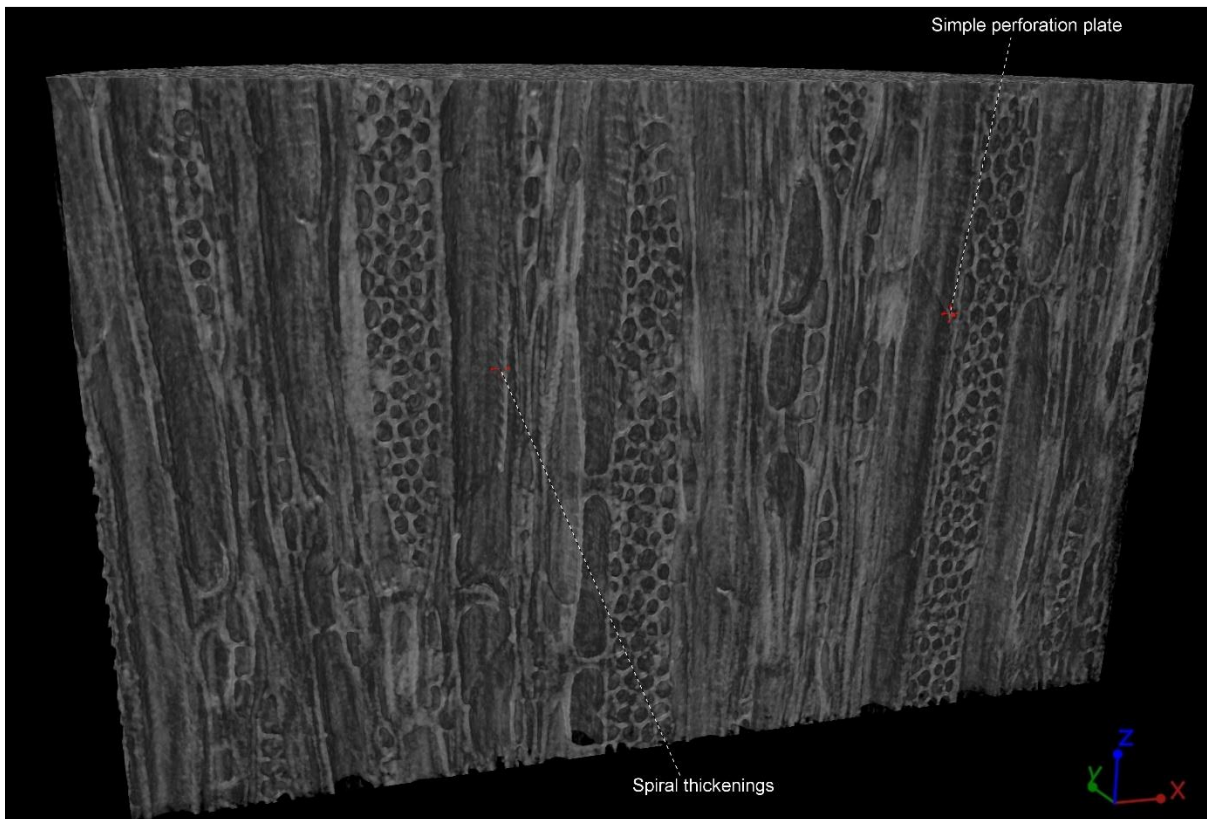
436 Figure 8. Post conservation (Versa) tuning peg Stage 3: TLS slice through the 'core'
437 region at 1 μm voxel resolution showing the multiseriate rays (up to 5 cells wide) and
438 occasional ray sheath cells indicated by the arrow.



439

440

441 Figure 9. Volume rendering (3D model) of the tuning peg 'core' showing the vessels'
442 spiral thickenings and simple perforation plates.



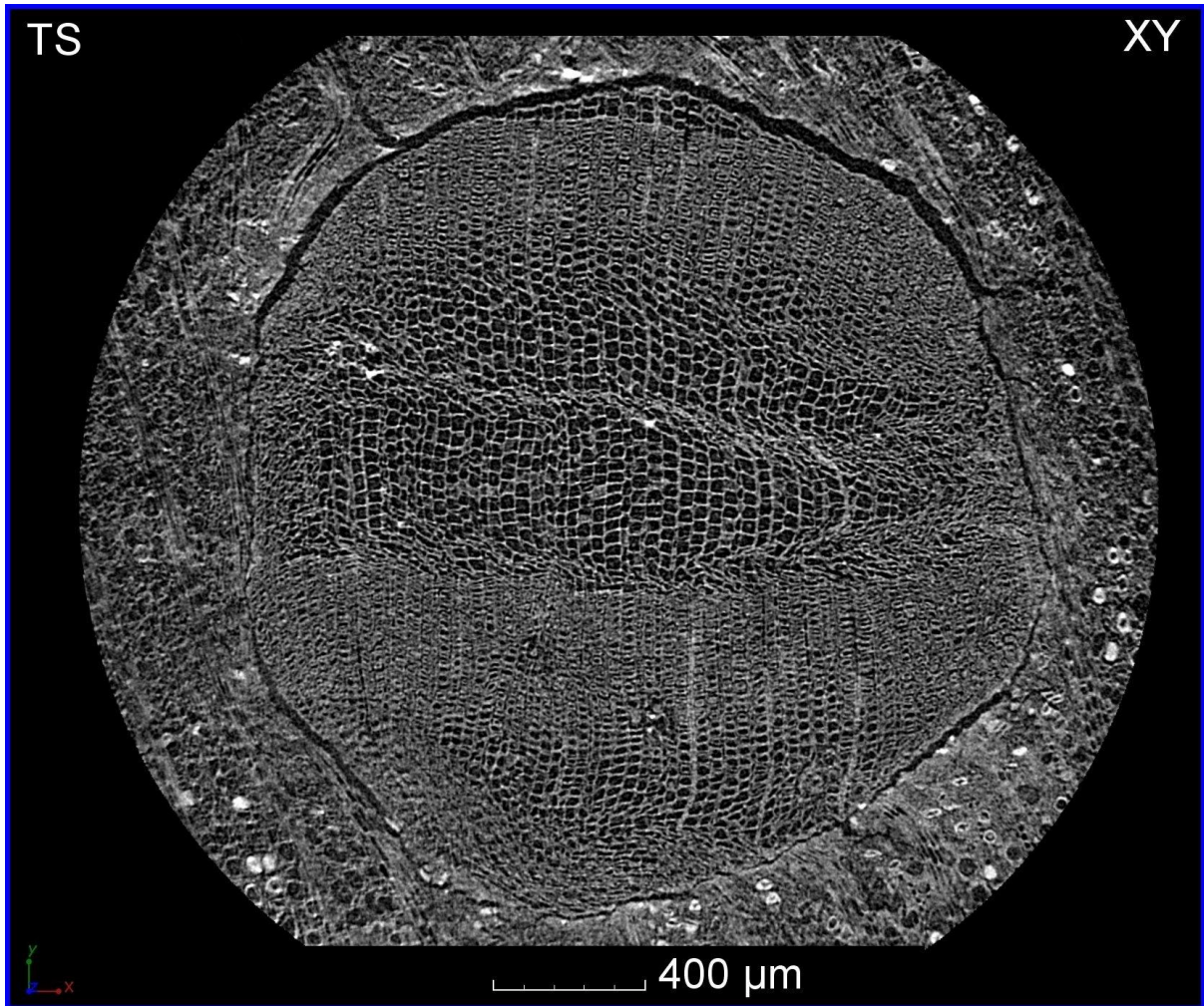
443
444

445 The tuning peg's cone insert coniferous identification was refined to *Pinus sylvestris*
446 (Scots pine) group with: i) sharp early-latewood boundary (Figure 10), ii) the
447 presence of both axial (Figure 10) and radial resin canals (Figure 11), iii) uniseriate
448 rays (here, typically ≤ 10 cells high, although a few were >10) (Figure 11), iv)
449 bordered pits (uniseriate alignment) in the axial tracheids (Figure 11), v) absence of
450 spiral thickenings, vi) window pits present in the ray cell walls (Figure 11), and vii)
451 the presence of dentate (tooth-shaped) features in the walls of the ray tracheids
452 (Figure 11). As well as *P. sylvestris* this (wood anatomical) group of taxa also
453 includes *Pinus mugo* (Dwarf mountain-pine) and *Pinus nigra* [consisting of two
454 subspecies, see Stace 2010] – none of which can be distinguished solely on the
455 basis of their wood anatomical characteristics (Schoch *et al* 2004, Schweingruber
456 1990)¹.

457

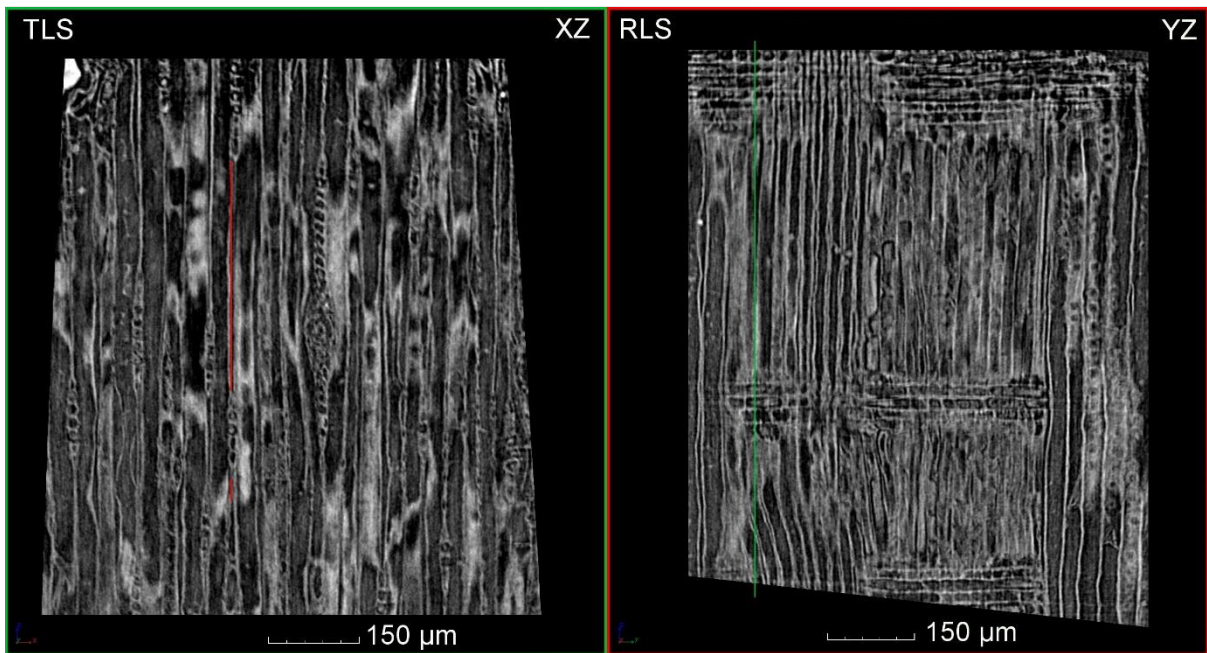
458 Figure 10. Post conservation (Versa) tuning peg Stage 1: TS slice image through the
459 softwood conical insert showing the abrupt early- to late-wood transition and axial
460 resin canal(s).

¹ Rol (1932) [in Phillips 1941, p. 294] defines the Sylvestris group (7) as including: *P. sylvestris*, and also *P. densiflora*, *P. nigra* and *P. resinosa*.



461
462

463 Figure 11. Post conservation (Versa) tuning peg Stage 3: slice images through the
464 softwood conical insert showing uniseriate rays (TLS), an axial resin canal (TLS),
465 single columns of bordered pits in the axial tracheids (RLS), window pits in the ray
466 cells (RLS) and dentate walls of the ray tracheids (RLS). The planar location of the
467 TLS slice (green border, right) is indicated by the corresponding colour line in the
468 RLS (red border, left) slice.



469
470
471
472
473
474
475
476
477
478

At least three separate growth rings were present, of which the third (i.e. youngest) ring was only very partial (radially). μ -CT also showed the poor condition of the insert, with radially distorted structure, evident as undulations in radially-aligned features that would originally have been linear, e.g. the rays. Whether this is due to the piece being compressed during manufacture, post-depositional decay, the conservation process itself, or a combination, is unclear.

4.3 Other general observations

479
480
481
482
483
484
485

As well as visualising the wood anatomical structure, μ -CT has also provided insights into the internal structure and condition of the objects. Scans showed a 'core' in the tuning peg body in better condition than the surrounding wood, without cracks and splits (Figure 12). The resulting clarity of the anatomical features enabled the secure wood identification.

486
487
488

Figure 12. Post conservation (HMX) tuning peg overview scan: TLS slice image showing the internal cracks and the inner 'core'. The blue lines indicate the points where the 'core' attaches (as determined in the TS plane).

TLS
1.0 mm

XZ



10 mm

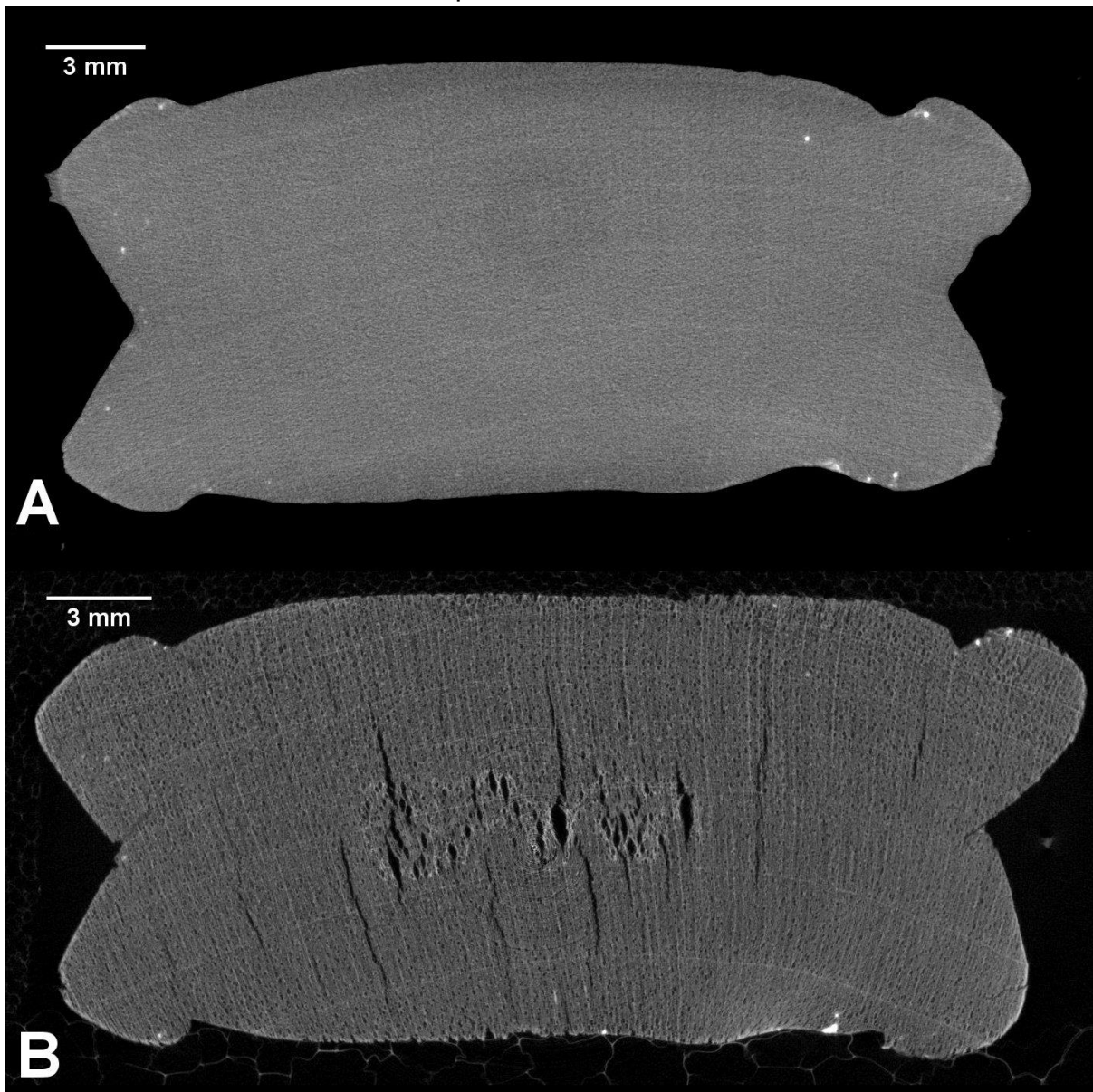


490

491 There is a horizontal crack through the peg at the point of the string hole and multiple
492 splits throughout the height (visible in Figures 7 and 12). These are lines of
493 weakness that will be vulnerable to breakage. Internal cracks are visible within the
494 pipe stopper too, manifesting as several radially aligned voids in the centre of its
495 head (Figure 13). It cannot be established whether these were present before
496 conservation due to the low CNR in the waterlogged object pre-conservation μ -CT
497 data. It is possible that PEG 400, which was used during the first stage of
498 impregnation, did not fully freeze and some air-drying took place in the very centre of
499 the pipe stopper resulting in cracks.

500

501 Figure 13. Pre- (A) versus post-conservation (B) (HMX) pipe stopper head overview
502 scan slices in the TS plane, show the limited contrast due to water content and
503 internal cracks that became visible post-conservation.



504

505

506 **4.4 Implications for future studies of waterlogged wooden objects**

507 Based on these results, if a wooden object is a candidate for conservation (using
508 PEG and freeze-drying) and destructive sampling is not desirable, there seems to be
509 little value in μ -CT scanning before conservation, especially as this study shows that
510 wood identifications are achievable on conserved material. As well as achieving high
511 contrast and resolution, scanning post-conservation also limits CT motion artefacts in
512 the reconstructed volumes (as water in objects can cause movement during the
513 scan) and lifts any restrictions on scan time due to concerns about wet objects drying
514 out.

515 μ -CT pre-conservation achieved limited image contrast in comparison to μ -CT post-
516 conservation, which made it difficult to resolve some features. Image contrast is
517 governed by variation in X-ray attenuation throughout the specimen. Figure 13
518 demonstrates how the contrast improves from a wet to a dry μ -CT scan (all that
519 differed in scanning set-up was the voltage –100 versus 80 kVp). On the ‘overview’
520 resolution scale, image contrast was more significant for identification of anatomical
521 features when comparing between pre-conservation and post-conservation μ -CT.
522 The Versa enabled phase-contrast edge enhancement from the fringe patterns
523 displayed at boundaries, which helped improve image fidelity and definition of
524 anatomical features in the vessel walls, such as perforation plates. The potential of
525 true phase-contrast lab-based microtomography of wood microstructure was
526 demonstrated by Mayo *et al* (2010), who also commented that weakly absorbing
527 thin-wall structures such as cell walls are more easily resolved. This could not be
528 trialled on the waterlogged objects due to scan time criteria to limit drying.

529 Post-conservation it was possible to achieve sub-micron resolution, and resolve
530 some of the finest anatomical features, including scalariform bars in the *Betula* sp.’s
531 perforation plates (typically $\sim 3 \mu\text{m}$ thick bars with $\sim 10 \mu\text{m}$ spacing) and the *Prunus*
532 sp.’s spiral thickenings on the vessel walls ($\sim 2 \mu\text{m}$). However, it should be minded
533 that the latter images were produced from the better-preserved ‘core’ of the tuning
534 peg. Even the highest resolution μ -CT (here 700 nm) could not fully resolve the tiny
535 individual pits in the vessels in the *Betula* sp.; the size criterion for minute pits is ≤ 4
536 μm (IAWA 1989, p. 250). When scanning at such high resolutions even the slightest
537 movements would cause misalignment of projection images, resulting in CT motion
538 artefacts in the reconstructed volumes, and necessitating a rigid specimen mount. A
539 stable mounting system was required for both scan-scenarios: before and after
540 conservation. However, there are limitations when mounting/stabilising very delicate
541 objects, as in the case of the tuning peg.

542 For this work, only two objects and three different wood types were available for
543 study and critical evaluation of μ -CT scanning as a technique for wood identification.
544 The results are promising and it is hoped that over time, wooden objects in
545 collections (which have been conserved in a similar way) that so far could not be
546 identified due to sampling restrictions, will be considered for wood identification to
547 add to our understanding of the use of wood as a resource to manufacture objects.

549 **4.5 Wood use and selection**

550 Three wood types have been securely identified to genus level: *Betula* sp. (birch)
 551 (pipe stopper), and *Prunus* sp. (cherries) and *Pinus sylvestris* (Scots pine) group
 552 (tuning peg). It is not appropriate to make detailed regionally-based inferences about
 553 likely species because the material was recovered from the wreck of an
 554 internationally travelled ship, although all the types have species that are native to
 555 the British Isles (see Stace 2010). Despite these reservations, some suggestion of
 556 possible wood source could be inferred when considered together with other
 557 evidence recovered from the ship; for example, the clay tobacco pipes themselves
 558 were typical of the London/southeast England region based on bowl typology of the
 559 mid-17th century (Higgins 2016), i.e. they were locally-produced and derived.

560

561 *Prunus* sp. “is strong, hard and has a close grain, and is excellent for turnery and
 562 carving” (Gale and Cutler 2000, p. 196), so its strength makes it well-suited for taking
 563 the strain of the instrument’s tightened string. In comparison, *Pinus sylvestris* (Scots
 564 pine) is relatively soft and easy to work, so more suitable for the decorative conical
 565 insert which was fitted and tightly-set within the peg’s body. Pine is pale-coloured,
 566 and therefore has the desired effect of being a striking visual comparison with the
 567 darker, red-brown coloured surrounding wood used for the body of the peg itself.
 568 As well as the wood types used, μ -CT has provided some insight on the construction
 569 of the objects; the tuning peg’s conical decorative insert, and the alignments of the
 570 wood grain. Although both objects have sections (the heads) where their width is
 571 greater than the depth, the wood alignments on these parts are different; the pipe
 572 stopper has the growth ring alignments parallel to the longest edge, and the tuning
 573 peg has the growth rings perpendicular to the longest edge.

574 **5 Summary and conclusions**

575 μ -CT has resulted in the better understanding of the internal structure of these
 576 wooden objects through i) the identification of wood type, ii) providing information on
 577 the manufacture techniques of the objects (in particular here, the alignment of wood
 578 grain, and use of a decorative component), and iii) identifying internal fractures and
 579 lines of weakness, vital for appropriate storage, handling and display. These data
 580 can be used to inform animations and museum displays, and create replica objects,
 581 for public engagement and education purposes.

582

583 Based on this study, the primary methodological recommendation is that, for wood
 584 identification purposes, μ -CT scanning is carried out on conserved wooden objects
 585 (i.e. not waterlogged remains). Ideally, scanning should be carried out at a range of
 586 voxel resolutions to assess anatomical features that range on multiple length scales
 587 e.g. growth rings (mm to cm), ray heights (μ m to mm) and pits in the vessel wall
 588 (μ m). Although the size of diagnostic features can vary between wood types (e.g.

589 the size of vessel pits), for the wood types encountered here 1 μm voxel resolution
 590 was sufficient to resolve the majority of anatomical features required for
 591 identification. 1 μm voxel resolution is advantageous from a scanning perspective as
 592 it enables the Versa 510's 4X objective to be used instead of the 20X; this improves
 593 the image intensity for a given exposure time so improves SNR or allows the
 594 exposure time, and thus scan time, to be reduced.

595
 596 $\mu\text{-CT}$ scanning requires specialist equipment and staff and can also be time
 597 consuming. The time [cost] available for undertaking the scans and manipulating the
 598 image data (as well as liaising with the wood and conservation specialists), needs to
 599 be weighed up against the 'knowledge gain' of additional information, and the
 600 importance and level of its contribution to understanding and valuing the objects.
 601 Table 3 sets out the cost/benefit considerations of this study. If destructive sampling
 602 for wood identification is permitted, then that will always be far more cost-effective.

603
 604 Table 3. Comparison of lab $\mu\text{-CT}$ and conventional techniques for the purpose of
 605 wood identifications, specific to this study.

$\mu\text{-CT}$ scanning	Conventional technique
Non-destructive	Destructive
3D internal inspection – arbitrary re-orientation to identify features of interest	2D surface slice – integrity reliant on wood condition
Large number of slices in one scan	Multiple sampling required
Isotropic sub-micron resolution is achievable with suitable specimen size	Optical magnification up to 400X
1 day	20 minutes
Very large digital archive (GB–TB)	Smaller digital archive [from microscope images] (kB–MB)

606
 607 The large amount of born-digital data produced through $\mu\text{-CT}$ studies can be
 608 immense, and as such requires adequate storage facilities for its security and
 609 longevity, in order to ensure compliance with the FAIR (Findable-Accessible-
 610 Interoperable-Reuseable) data principles (Wilkinson *et al* 2016). This will have
 611 further cost implications.

612
 613 This work has successfully demonstrated the role and applications of $\mu\text{-CT}$ scanning
 614 complete, conserved (previously waterlogged) wooden objects, and how best to use
 615 the technique, when destructive sampling and/or other imaging techniques (e.g.
 616 Synchrotron) are not appropriate/accessible. It shows that the impregnation of PEG
 617 together with freeze-drying do not obscure the anatomical features of wood up to the
 618 resolutions achieved in this study (for these species), and that successful wood
 619 identifications are possible on wooden material conserved in this way.

620

621 **6 References**

622

623 Barbour, RJ 1990 'Treatments for waterlogged and dry archaeological wood', in: RM
624 Rowell and RJ Barbour (ed.s) *Archaeological wood: properties, chemistry and*
625 *preservation*. Washington, DC: American Chemical Society, 177–194

626

627 Barrett, JF and Keat, N 2004 'Artifacts in CT: Recognition and avoidance'
628 *RadioGraphics* 24, 1679–1691

629

630 Bird, MI, Ascough, PL, Young, IM, Wood, CV and Scott, AC 2008 'X-ray
631 microtomographic imaging of charcoal' *Journal of Archaeological Science* 35, 2698–
632 2706

633

634 British Standards Institute (2012) BS EN 16085:2012 - *Conservation of Cultural*
635 *property: Methodology for sampling from materials of cultural property: General*
636 *rules*, [Np.p.]: BSI

637

638 Cartwright, C 2015 'The principles, procedures and pitfalls in identifying
639 archaeological and historical wood samples' *Annals of Botany* 116(1), 1–13

640

641 Cronyn, JM 1990 *The elements of archaeological conservation* London: Routledge

642

643 Fioravanti, M, DiGiulio, G and Signorini, G 2017 'A non-invasive approach to
644 identifying wood species in historical musical instruments' *Journal of Cultural*
645 *Heritage* 27 Supplement, S70–S77

646

647 Flink, JM and Knudsen, H 1983 *An introduction to freeze drying*. Denmark:
648 Strandberg Bogtryk

649

650 Gale, R and Cutler, D 2000 *Plants in archaeology: identification manual of artefacts*
651 *of plant origin from Europe and the Mediterranean*. Otley: Westbury Publishing

652

653 Grabner, M, Salaberger, D and Okochi, T 2009 'The Need of High Resolution μ -X-
654 ray CT in Dendrochronology and in Wood Identification' *Proceedings of 6th*
655 *International Symposium on Image and Signal Processing and Analysis* 16–18
656 September 2009, Salzburg, Austria [10.1109/ISPA.2009.5297695](https://doi.org/10.1109/ISPA.2009.5297695)

657

658 Haneca, K, Deforce, K, Boone, M, Van Loo, D, Dierick, M, Van Acker, J and Van den
659 Bulcke, J 2012 'X-ray sub-micron tomography as a tool for the study of
660 archaeological wood preserved through the corrosion of metal objects' *Archaeometry*
661 54, 893–905

662

663 Hazell, Z and Aitken, E 2019 *The London protected wreck, The Nore, off Southend-*
664 *on-Sea, Thames Estuary, Essex: Wood identifications and recording of wooden*
665 *remains recovered between 2014 and 2016* Historic England Research Report
666 Series 15/2019
667

668 Heacock, B, Sarenac, D, Cory, DG, Huber, MG, Maclean, JPW, Miao,
669 H, Wen, H and Pushin, DA 2020 'Neutron sub-micrometre tomography from
670 scattering data' *International Union of Crystallography Journal* 7, 893–900
671

672 Hervé, V, Mothe, F, Freyburger, C, Gelhaye, E and Frey-Klett, P 2014 'Density
673 mapping of decaying wood using X-ray computed tomography' *International*
674 *Biodeterioration and Biodegradation* 86, 358–363
675

676 Higgins, DA 2016 *Clay tobacco pipe and stoppers* Unpublished specialist report for
677 Cotswold Archaeology and Historic England
678

679 Hocker, E 2018 *Preserving Vasa*. Archetype Publications Ltd, in association with
680 Vasa Museum, Stockholm
681

682 Hoffman, P 2013 *Conservation of Archaeological Ships and Boats*. Archetype
683 Publications Ltd, in association with Deutsches Schiffahrtsmuseum
684

685 Hubau, W, Van den Bulcke, J, Kitin, P, Brabant, L, Van Acker, J and Beeckman, H
686 2013 'Complementary imaging techniques for charcoal examination and
687 identification' *IAWA Journal* 34(2), 147–168
688

689 IAWA 1989 'IAWA list of microscopic features for hardwood identification: with an
690 appendix on non-anatomical identification' *IAWA Bulletin* 10(3), 219–332. By a
691 Committee of the International Association of Wood Anatomists, (ed.s) Wheeler, EA,
692 Baas, P and Gasson, PE
693

694 Jones, M. (ed.) 2003 *For Future Generations. Conservation of a Tudor maritime*
695 *collection. The Archaeology of the Mary Rose*. Volume 5. Portsmouth: The Mary
696 Rose Trust Ltd

697 Kanazawa, Y, Yamada, T, Kido, A, Fujimoto, K, Takakura, K, Hayashi, H, Fushimi,
698 Y, Kozawa, S, Koizumi, K, Okuni, M, Ueda, N and Togashi, K 2017 'Internal
699 evaluation of impregnation treatment of waterlogged wood; relation between
700 concentration of internal materials and relaxation time using magnetic resonance
701 imaging' *Magnetic Resonance Imaging* 38, 196–201
702

703 Kowalczyk, J, Rachocki, A, Broda, M, Mazela, B, Ormondroyd, GA and Tritt-Goc,
704 J 2019 'Conservation process of archaeological waterlogged wood studied by

705 spectroscopy and gradient NMR methods' *Wood Science and Technology* 53, 1207–
706 1222
707

708 Landis, EN and Keane, DT 2010 'X-ray microtomography' *Materials characterization*
709 61, 1305–1316
710

711 Lehmann, E, Hartmann, S, and Wyer, P 2005 'Neutron radiography as visualization
712 and quantification method for conservation measures of wood firmness
713 enhancement' *Nuclear Instruments and Methods in Physics Research, Section A:*
714 *Accelerators, Spectrometers, Detectors and Associated Equipment* 542(1–3), 87–94
715

716 Mannes, D, Marone, F, Lehmann, E, Stampanoni, M and Niemz, P 2010 'Application
717 areas of synchrotron radiation tomographic microscopy for wood research' *Wood*
718 *Science and Technology* 44, 67–84
719

720 Mayo, SC, Chen, F, and Evans, R 2010 'Micron-scale 3D imaging of wood and plant
721 microstructure using high resolution X-ray phase-contrast microtomography' *Journal*
722 *of Structural Biology* 171, 182–188
723

724 Mizuno, S, Torizu, R and Sugiyama, J 2010 'Wood identification of a wooden mask
725 using synchrotron X-ray microtomography' *Journal of Archaeological Science* 37(11),
726 2842–2845
727

728 Morales, S, Guesalaga, A, Fernández, MP, Guarini, M, and Irrarázaval, P 2004
729 'Computer reconstruction of pine growth rings using MRI' *Magnetic Resonance*
730 *Imaging* 22(3), 403–412
731

732 Mori, M, Kuhara, S, Kobayashi, K, Suzuki, S, Yamada, M and Senoo, A 2019 'Non-
733 destructive tree-ring measurements using a clinical 3T-MRI for archaeology'
734 *Dendrochronologia* 57, Article 125630
735

736 O'Connor, S 2007 'High definition X-radiography of textiles: methods and
737 approaches' in (ed.s) S O'Connor and MM Brooks *X-radiography of Textiles, Dress*
738 *and related Objects* London: Butterworth-Heinemann, 23–57
739

740 Phillips, EWJ 1941 'The identification of coniferous woods by their microscopic
741 structure' *Journal of the Linnean Society of London, Botany* 52(343), 259–320
742

743 Quye, A and Strlič, M 2019 *Ethical Sampling Guidance* Icon Heritage Science
744 Group, January 2019 [https://www.icon.org.uk/resource/ethical-sampling-](https://www.icon.org.uk/resource/ethical-sampling-guidance.html)
745 [guidance.html](https://www.icon.org.uk/resource/ethical-sampling-guidance.html)
746

747 Schoch, W, Heller, I, Schweingruber, FH and Kienast, F 2004 *Wood anatomy of*
748 *central European Species* Online version: www.woodanatomy.ch accessed 28
749 January 2020
750

751 Schweingruber, F 1990 *Microscopic Wood Anatomy: structural variability of stems*
752 *and twigs in recent and subfossil woods from central Europe*. Birmensdorf: Swiss
753 Federal Institute of Forestry Research
754

755 Stace, C 2010 *New Flora of the British Isles* Third edition. Cambridge: Cambridge
756 University Press, 3rd printing
757

758 Stelzner, J and Million, S 2015 'X-ray Computed Tomography for the anatomical and
759 dendrochronological analysis of archaeological wood' *Journal of Archaeological*
760 *Science* 55, 188–196
761

762 Steppe, K, Cnudde, V, Girard, C, Lemeur, R, Cnudde, J-P and Jacobs, P 2004 'Use
763 of X-ray computed microtomography for non-invasive determination of wood
764 anatomical characteristics' *Journal of Structural Biology* 148, 11–21
765

766 Tazuru, S and Sugiyama, J 2019 'Wood identification of Japanese Shinto deity
767 statues in Matsunoo-taisha Shrine in Kyoto by synchrotron X-ray microtomography
768 and conventional microscopy methods' *Journal of Wood Science* 65, Article 60
769

770 Van den Bulcke, J, Masschaele, B, Dierick, M, Van Acker, J, Stevens, M and Van
771 Hoorebeke, L 2008 'Three-dimensional imaging and analysis of infested coated
772 wood with X-ray submicron CT' *International Biodeterioration & Biodegradation* 61,
773 278–286
774

775 Van den Bulcke, J, Van Loo, D, Dierick, M, Masschaele, B, Van Hoorebeke, L and
776 Van Acker, J 2017 'Nondestructive research on wooden musical instruments: From
777 macro- to microscale imaging with lab-based X-ray CT systems' *Journal of Cultural*
778 *Heritage* 27 Supplement, S78–S87
779

780 Walsh, M (ed.) with Aitken, E, Allen, SJ, Armitage, PL, Baker, P, Brown, DH,
781 Campbell, G, Endors, R, Garside, P, Gleba, M, Grant, M, Higgins, DA, Hazell, Z,
782 Hildred, A, Mays, S, Middleton, A, Miller, Z, Mould, Q, Panter, I, Pascoe, D, Pawson,
783 D, Paynter, S, Schuster, J, Ströbele, F, Marsden, K, Rankin, K, Ströbele, F, Taylor,
784 M, Turner-Walker, G and Wyles, S. Forthcoming. *The wreck of the London:*
785 *Archaeological investigations of a 17th-century warship*. Cotswold Archaeology
786 Monograph. Cotswold Archaeology / Historic England.
787

788 Wei, Q, Leblon, B and La Rocque, A 2011 'On the use of X-ray computed
789 tomography for determining wood properties: a review' *Canadian Journal of Forest*
790 *Research* 41(11), 2120–2140

791
792 Wilkinson, MD, Dumontier, M, Aalbersberg, IJ, Appleton, G, Axton, M, Baak, A,
793 Blomberg, N, Boiten, J-W, Bonino da Silva Santos, L, Bourne, PE, Bouwman, J,
794 Brookes, AJ, Clark, T, Crosas, M, Dillo, I, Dumon, O, Edmunds, S, Evelo, CT,
795 Finkers, R, Gonzalez-Beltran, A, Gray, AJG, Groth, P, Goble, C, Grethe, JS,
796 Heringa, J, 't Hoen, PAC, Hooft, R, Kuhn, T, Kok, R, Kok, J, Lusher, SJ, Martone,
797 ME, Mons, A, Packer, AL, Persson, B, Rocca-Serra, P, Roos, M, van Schaik, R,
798 Sansone, S-A, Schultes, E, Sengstag, T, Slater, T, Strawn, G, Swertz, MA,
799 Thompson, M, van der Lei, J, van Mulligen, E, Velterop, J, Waagmeester, A,
800 Wittenburg, P, Wolstencroft, K, Zhao, J and Mons, B 2016 'The FAIR Guiding
801 Principles for scientific data management and stewardship' *Scientific Data* 3, 160018
802

803 **7 Acknowledgements**

804 KER and MNM undertook the μ -CT scanning, with KER carrying out the image
805 processing, ZJH carried out the wood identifications and recording, and AMM
806 recorded and conserved the archaeological artefacts. The photographs of the
807 conserved objects were taken by James Davies (Lead Photographer) and Steven
808 Baker (Photographer) (both Historic England).

809

810 Many thanks to the following organisations and individuals:

- 811 - the wreck's licensee Steve Ellis, together with Carol Ellis, Steve Meddle and
812 the licensee team
- 813 - Historic England for funding project Pr6901 and supporting this additional
814 research
- 815 - Cotswold Archaeology for managing project Pr6901
- 816 - MSDS Marine who provided diving support for the excavation
- 817 - Dan Pascoe, the site nominated archaeologist (2014-2016)
- 818 - the μ -VIS X-Ray Imaging Centre, University of Southampton, for allocating
819 the staff and resources to carry out this study, supported by EPSRC grant
820 EP-H01506X. Special thanks to Richard Boardman.

821 The project archive will be deposited with the ADS and Southend Museum Services.
822 The pipe stopper is currently loaned to, and on display at, the National Maritime
823 Museum, Greenwich, London. Supporting CT data are openly available from the
824 University of Southampton repository at <https://doi.org/10.5258/SOTON/D1940>.
825 Contact the corresponding author for raw imaging data.

826

827 <https://historicengland.org.uk/advice/heritage-at-risk/search-register/list-entry/24507>

828

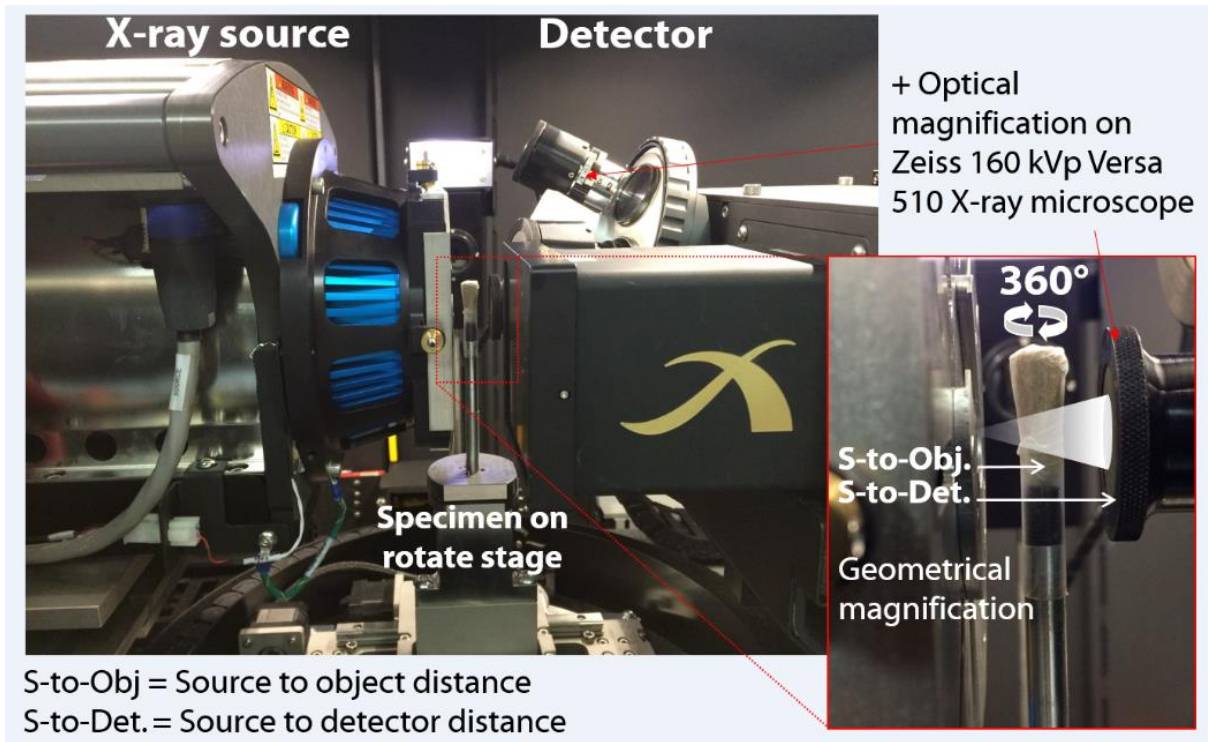
829 #LondonWreck1665

830

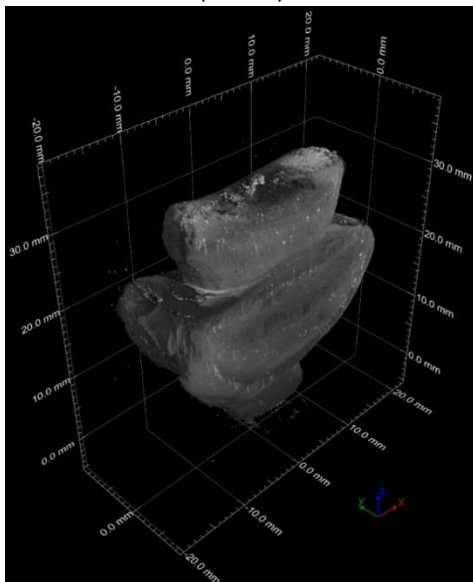
831 Finally, many thanks to the anonymous reviewers for their constructive feedback and
832 recommendations.

833 **8 Appendix**

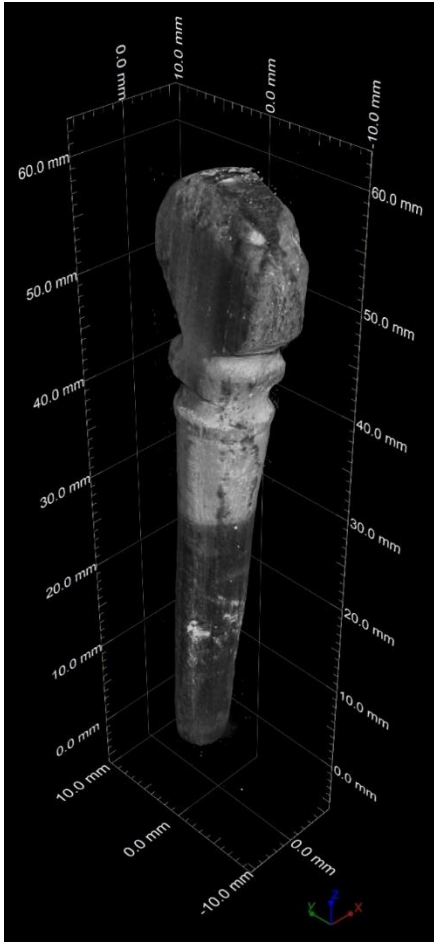
834 Figure A1. The object (here, shaft of the pipe stopper) was mounted for μ -CT
835 scanning with two stage magnification within the Versa to achieve sub-micron
836 resolution.



838 Figure A2. μ -CT volume rendering (3D model) of the pipe stopper head, before
839 conservation (HMX).



840
841
842 Figure A3. μ -CT volume rendering (3D model) of the tuning peg, before conservation
843 (HMX).



844
845